PriMera Scientific Surgical
Research and Practice
Volume 8 Issue 2 August 2026
DOI: 10.56831/PSSRP-08-320
ISSN: 2836-0028

PriMera Scientific Publications

Bircotebs - A Bilateral Radiographic-Stochastic Model for the Complementary States (Health/Disease) of the D-Organ and Middle-Ear Mucosa

Type: Research Article
Received: June 30, 2026
Published: August 04, 2026

Citation:
Adela-Ioana Mocanu., et al. "*Bircotebs* - A Bilateral Radiographic-Stochastic Model for the Complementary States (Health/Disease) of the D-Organ and Middle-Ear Mucosa". PriMera Scientific Surgical Research and Practice 8.2 (2026): 207-228.

Copyright:
© 2026 Adela-Ioana Mocanu., et al. This is an open-access article distributed under the Creative Commons Attribution License, which permits unrestricted use, distribution, and reproduction in any medium, provided the original work is properly cited.

Marian Radulescu[1], Adela-Ioana Mocanu[2,3]*, Mihai Lupascu[4,5]*, Vasile Lungu[6§], Mihai-Adrian Schipor[7] and Horia Mocanu[8,9]

[1]Department of ENT&HNS, Faculty of Medicine, "Carol Davila" University of Medicine and Pharmacy, 020021, Bucharest, Romania

[2]Doctoral School, Faculty of Medicine, "Titu Maiorescu" University, 031593 Bucharest, Romania

[3]Department of ENT&HNS, Gaesti City Hospital, 135200, Gaesti, Dambovita, Romania

[4]Department of ENT&HNS, Faculty of Medicine, "Ovidius" University, 900527, Constanta, Romania

[5]Department of ENT&HNS, Constanta County Clinical Emergency Hospital, 900591, Constanta, Romania

[6]Department of General Surgery, Ilfov County Clinical Emergency Hospital; 022104, Bucharest, Romania

[7]Technical University of Munich, Institute of Astronomical and Physical Geodesy, 80333 Munich, Germany

[8]Department of ENT&HNS, Faculty of Medicine, "Titu Maiorescu" University, 031593, Bucharest, Romania

[9]Department of ENT&HNS, Ilfov County Clinical Emergency Hospital; 022104, Bucharest, Romania

***Corresponding Authors:** Adela-Ioana Mocanu, Doctoral School, Faculty of Medicine, "Titu Maiorescu" University, 031593 Bucharest, Romania; Department of ENT&HNS, Gaesti City Hospital, 135200, Gaesti, Dambovita, Romania.

*Mihai Lupascu, Department of ENT&HNS, Faculty of Medicine, "Ovidius" University, 900527, Constanta, Romania; Department of ENT&HNS, Constanta County Clinical Emergency Hospital, 900591, Constanta, Romania.

§Contributed Equally: Vasile Lungu, Department of General Surgery, Ilfov County Clinical Emergency Hospital; 022104, Bucharest, Romania.

Abstract

The suppuration of the middle-ear (ME) is a common pathology (over 20 million individuals for chronic suppuration only, according to latest reports by the WHO) facilitated by the notoriously complicated and irregular anatomic structure ot the temporal bone (TB). Clinically, the patients experience frequent recurrences and over 50% of subjects suffer from conductive hearing

loss. The geometry of the mastoid air cells system (MACS) has not been described for adults over a large range of MACS volumes. The volume of this complicated system of interconnected air cells is difficult to measure and current studies tend to suggest that MACS and not the Eustachian tube opening is the primary gas source for the ME. The bony walls of these cavities are radiopaque and form the bony support for the *D-Organ* that we have previously defined along with the Unilateral Radiographic-Stochastic Model for its Complementary States (Health/Disease). The aim of the current study is to provide a correct and complete approach to the previously mentioned fields of research which implies the analysis of the *D-Organ* as a pair (a pair of middle-ears). This is reflected in the **BI**lateral **R**adiographic **CO**nformation of the **TE**mporal **B**one in Schuller projection (**BIRCOTEBS**). We aim to continue our research and to tap the considerable potential of this statistic-probabilistic perspective on the phenomena and processes of interest regarding the structure and function of the ME, both in normal and pathological conditions. From a statistical and probabilistic point of view, the **BIRCOTEBS** is a natural development and continuation of our analysis of the **URCOTEBS**. This data is encoded within the image and we aim to decode and translate it into clinical data for a bilateral approach this time. The present work gives, through stochastic methods, the key to decoding this information into clinical language. This **nosographic-radiographic-stochastic** model (both in theory and in practice - the patient's radiography) represents a necessary but not sufficient step in defining all aspects of chronic ME disease. This radiographic system is readily available and clinically usable.

Keywords: radiology; X-rays; tomography; otitis media; ventilation; anatomy; physiology; statistical modeling

Introduction

Our previous work in defining the *D-Organ* as an unistratified epithelial cellular population of homogenous morphology supported by a basilar membrane on top of a conjunctive structure that provides vascularization and innervation along with the **URCOTEBS** (**U**nilateral **R**adiographic **CO**nformation of the **TE**mporal **B**one in **S**chuller projection), has presented in full the arguments for the URCOTEBS as being a codified visiting card for the two complementary states: functional (Healthy) or non-functional (Diseased) of the Middle Ear (ME) (1). In other words, discussing the *D-Organ* as a one-of-a-kind organ is necessary but not sufficient to explain the epidemiology, nosography, pathology and clinical manifestation of the *Chronic Inflammation of the ME Mucosa* (1, 2, 3).

We have previously defined the *D-Organ* as a unistratified epithelial cellular population of homogenous morphology supported by a basilar membrane on top of a con-junctive structure that provides vascularization and innervation. The subjacent bone structure is known as the *Variable Geometry Anatomic Macroscopic Radiopaque Peripheral Support of the D-Organ*. This bony structure is geometrically arranged as irregular interlinked spheroidal and polyhedric cavities which form a common enclosure of completely determined volume V_{ε}. [1-3]. Through purely theoretical calculation and anatomical measurements we have created an accurate description of two previously un-defined organs, D and F.

The F-Organ represents a passive surface element for the diffusion of respiratory gases whilst the *D-Organ* actively pumps, within the same time interval, the same quantity of gas mix diffused through the F-Organ so that the mass and total pressure of the gas mix inside the ME remain constant. A simpler, more medical approach would be: *the first functional area* (*F-Organ*) is a surface of gas diffusion from the ME to the internal environment of the body, determined by gradient of partial pressures of respiratory gases on both sides of the epithelium (this role is currently unanimously accepted for the entire mucosa of the ME); *the second functional area* (*D-Organ*) acts as a biological pump, consuming metabolic energy, with an efficiency situated at the upper limit of a biological systems and that has dynamics and cinematics explainable by a physical-mathematical model [3].

A correct and complete approach to the previously mentioned fields of research implies the analysis of the *D-Organ* as a pair (a pair of middle-ears). This is reflected in the **BI**lateral **R**adiographic **CO**nformation of the **TE**mporal **B**one in **S**chuller projection (**BIRCOTEBS**). From a statistical and probabilistic point of view, the **BIRCOTEBS** is a natural development and continuation of our analysis of the **URCOTEBS** [1-3].

From a geometric, stochastic and radiologic perspective the *D-Organ* represents the sum of all *D-Cells* or the Static General Population of *D-Cells*. Axiomatically we consider that the D-Cell can only be in one of the two complementary states: functional (Healthy) or non-functional (Diseased) [1-3].

The bilateral radiographic examination of the temporal bone (mastoid) in Schuller projection, similar to the unilateral examination, results in an overlapping projection of all bony cavities that comprise the *General Endo-temporal Bony Cavity Complex* onto the same plain (film) and this constitutes an advantage from the multiple CT sections because the set of stochastic information is found in the whole of the cavities taken as one. The decoding must be done accordingly, only this time for both mastoid bones concomitantly and this occurs much faster with conventional radiography [1-3].

Methods Used

Transferring the discussion from **URCOTEBS** to **BIRCOTEBS** can only be done through combinatorics and probability calculus. In other words, having defined the manifestations and appearance of **URCOTEBS** (Table I & II), by applying the aforementioned mathematical instruments, we aim to determine the ways of expression of **BIRCOTEBS** (Tables III & Figure 1). The stochastic basis for this type of diagnostic tool is founded on the existence of the *D-Organ* and the definition of **URCOTEBS**, which have never before been presented in literature. Understanding our present work requires understanding our previous articles and especially the terminology. This is sometimes understandably challenging as the research in not primarily oriented towards clinicians but rather researchers in the fields of physiology, physics, mathematics, statistics etc.

The entire statistic methodology based on the unreplaced ball principle, also known as hypergeometric distribution and Poisson's Scheme has been in our previous work extensively presented [1].

The measurements used for defining both the **URCOTEBS** and **BIRCOTEBS** systems have been done on simple X-rays (Schuller's view) as presented in Table II. The decoding occurs much fasters using this two-dimensional system (conventional radiography) This image of the TB in Schuller's projection is a mirror that reflects the status of the ME mucosa, and **URCOTEBS** encodes the physiological state of the *D-Organ*. In ascending order of their projection areas (projection of their Variable Geometry Peripheral Endo-temporal Bony Cavity Complex) we can organize the following:

Generic URCOTEBS symbol	***Probability of URCOTEBS (The unreturned ball principle and Poisson's scheme)[1]***	***Specific URCOTEBS symbol [1] Disease***	***Probability of Disease[1]***	***Specific URCOTEBS symbol [1] Health***	***Probability of Helth[1]***
a	59.7%	*Alfa* α	0.60%	**A**	99.40%
b	0.8%	*Beta* β	1.40%	**B**	98.60%
c	13.3%	*Gamma* γ	7.90%	**C**	92.10%

Table 1: Unilateral Radiographic Conformations – URCOTEBS(1)– with corresponding informations. Each URCOTEBS species represents a randomized exclusive event of determined achievement probability.

a	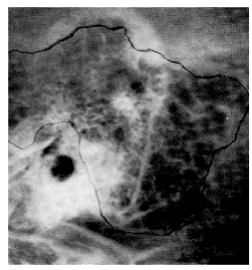

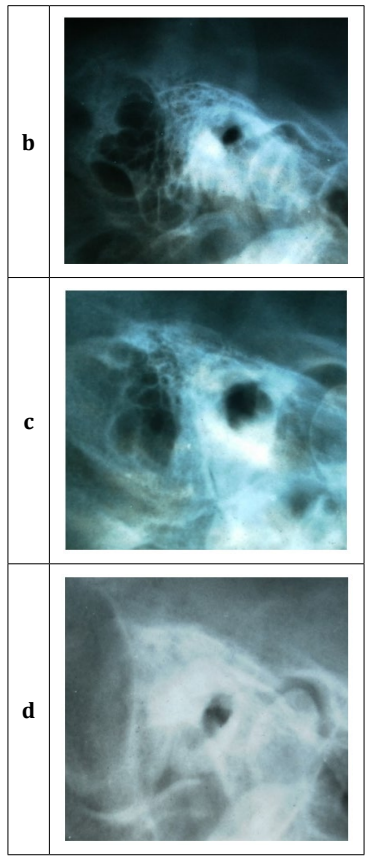

Table 2: Unilateral Radiographic Conformations – URCOTEBS (1).

URCOTEBS Index	*Generic URCOTEBS symbol*	*Probability of URCOTEBS (1) (The unreturned ball principle and Poisson's scheme) (1)*	*URCOTEBS Index*	*Generic URCOTEBS symbol*	*Probability of URCOTEBS (1) (The unreturned ball principle and Poisson's scheme) (1)*	*Generic URCOTEBS symbol*	*Product of URCOTEBS probabilities (Corrected – brought to 100%) (1)*	*URCOTEBS Index*	*Generic URCOTEBS symbol*
1	**a**	0.597	1	**a**	0.597	**a ~ a**	0.4943	1	a ~ a
1	**a**	0.597	2	**b**	0.00754	**a ~ b**	0.0062	2	a ~ b
1	**a**	0.597	3	**c**	0.133	**a ~ c**	0.1101	3	a ~ c
1	**a**	0.597	4	**d**	0.262	**a ~ d**	0.217	4	a ~ d
2	**b**	0.00754	2	**b**	0.00754	**b ~ b**	0.0001	5	b ~ b
2	**b**	0.00754	3	**c**	0.133	**b ~ c**	0.0014	6	b ~ c
2	**b**	0.00754	4	**d**	0.262	**b ~ d**	0.0027	7	b ~ d
3	**c**	0.133	3	**c**	0.133	**c ~ c**	0.0245	8	c ~ c
3	**c**	0.133	4	**d**	0.262	**c ~ d**	0.0483	9	c ~ d
4	**d**	0.262	4	**d**	0.262	**d ~ d**	0.0953	10	d ~ d
Sum of Probabilities							1.0000		

Table 3: Types of manifestation of BIRCOTEBS – and their genesis from possible combinations of manifestations of URCOTEBS.

URCOTEBS Index	*Generic URCOTEBS symbol*	*Specific URCOTEBS symbol*	*Probability of. URCOTEBS Disease/Health (relative frequency)*	*BIRCOTEBS Index*	*Generic URCOTEBS symbol*	*Specific URCOTEBS symbol*	*Probability of. URCOTEBS Disease/Health (relative frequency)*	*Prodct of relative frequencies of URCO-TEBS Disease/Health (col. IV & col.VIII)*	*Generic BIRCOTEBS symbol*	*Specific BIRCOTEBS symbol Disease/ Health*
I	II	III	IV	V	VI	VII	VIII	IX	X	XI
1	a	a	0.0195	1	a	a	0.0195	0.0004	a ~ a	a ~ a
1	a	a	0.0195	5	a	A	0.98	0.0191	a ~ a	a ~ A
5	a	A	0.98	5	a	A	0.98	0.961	a ~ a	A ~ A
1	a	a	0.0195	2	b	b	0.0731	0.0014	a ~ b	a ~ b
1	a	a	0.0195	6	b	B	0.927	0.0181	a ~ b	a ~ B
5	a	A	0.98	6	b	B	0.927	0.909	a ~ b	A ~ B
1	a	a	0.0195	3	c	g	0.18	0.0035	a ~ c	a ~ g
1	a	a	0.0195	7	c	C	0.82	0.016	a ~ c	a ~ C
5	a	A	0.98	7	c	C	0.82	0.804	a ~ c	A ~ C
1	a	a	0.0195	4	d	d	1	0.0195	a ~ d	a ~ d
2	b	b	0.0731	5	a	A	0.98	0.0717	b ~ a	b ~ A
2	b	b	0.0731	2	b	b	0.0731	0.0053	b ~ b	b ~ b
2	b	b	0.0731	6	b	B	0.927	0.0678	b ~ b	b ~ B
6	b	B	0.927	6	b	B	0.927	0.859	b ~ b	B ~ B
2	b	b	0.0731	3	c	g	0.18	0.0131	b ~ c	b ~ g
2	b	b	0.0731	7	c	C	0.82	0.06	b ~ c	b ~ C
6	b	B	0.927	7	c	C	0.82	0.76	b ~ c	B ~ C
2	b	b	0.0731	4	d	d	1	0.0731	b ~ d	b ~ d
3	c	g	0.18	5	a	A	0.98	0.176	c ~ a	g ~ A
3	c	g	0.18	6	b	B	0.927	0.167	c ~ b	g ~ B
3	c	g	0.18	3	c	g	0.18	0.0323	c ~ c	g ~ g
3	c	g	0.18	7	c	C	0.82	0.148	c ~ c	g ~ C
7	c	C	0.82	7	c	C	0.82	0.673	c ~ c	C ~ C
3	c	g	0.18	4	d	d	1	0.18	c ~ d	g ~ d
4	d	d	1	5	a	A	0.98	0.98	d ~ a	d ~ A
4	d	d	1	6	b	B	0.927	0.927	d ~ b	d ~ B
4	d	d	1	7	c	C	0.82	0.82	d ~ c	d ~ C
4	d	d	1	4	d	d	1	1	d ~ d	d ~ d

Table 4: Bilateral Radiographic Conformations BIRCOTEBS – genesis of combinations of Disease and Health.

Current BIRCOTEBS Index	*BIRCOTEBS Index*	*Probabilities of Exclusive BIRCOTEBS Events(Product of Probabilities of Exclusive URCOTEBS Events)* [1] [1]	*Generic BIRCOTEBS symbol*	*Specific BIRCOTEBS symbol Disease/ Health*	*Product of relative URCOTEBS frequencies Disease/Health*	*Probability of Exclusive .BIRCOTEBS Event Disease/Health (product of col. III & col. VI)*
I	II	III	IV	V	VI	VII
1	1	0.4943	a ~a	a ~ a	0.0004	0.000191
2	1	0.4943	a ~ a	a ~ A	0.0191	0.00959
3	1	0.4943	a ~ a	A ~ A	0.961	0.481
4	2	0.0062	a ~ b	a ~ b	0.0014	0.000009
5	2	0.0062	a ~ b	a ~ B	0.0181	0.000114
6	2	0.0062	a ~ b	A ~ B	0.909	0.00575
7	2	0.0062	b ~ a	b ~ A	0.0717	0.000453
8	3	0.1101	a ~ c	a ~ g	0.0035	0.000392
9	3	0.1101	a ~ c	a ~ C	0.016	0.00179
10	3	0.1101	a ~ c	A ~ C	0.804	0.0897
11	3	0.1101	c ~ a	g ~ A	0.176	0.0197
12	4	0.217	a ~ d	a ~ d	0.0195	0.00429
13	4	0.217	d ~ a	d ~ A	0.98	0.216
14	5	0.0001	b ~ b	b ~ b	0.0053	0
15	5	0.0001	b ~ b	b ~ B	0.0678	0.000005
16	5	0.0001	b ~ b	B ~ B	0.859	0.000069
17	6	0.0014	b ~ c	b ~ g	0.0131	0.000019
18	6	0.0014	b ~ c	b ~ C	0.06	0.000085
19	6	0.0014	b ~ c	B ~ C	0.76	0.00107
20	6	0.0014	c ~ b	g ~ B	0.167	0.000235
21	7	0.0027	b ~ d	b ~ d	0.0731	0.000203
22	7	0.0027	d ~ b	d ~ B	0.927	0.00257
23	8	0.0245	c ~ c	g ~ g	0.0323	0.000804
24	8	0.0245	c ~ c	g ~ C	0.148	0.00367
25	8	0.0245	c ~ c	C ~ C	0.673	0.0167
26	9	0.0483	c ~ d	g ~ d	0.18	0.00881
27	9	0.0483	d ~ c	d ~ C	0.82	0.0402
28	10	0.0953	d ~ d	d ~ d	1	0.0965
Sum of probabilities						1,0000

Table 5: Bilateral Radiographic Conformations (BIRCOTEBS); genesis of Probabilities (Prevalence) of Randomized Exclusive Events meaning Complementary States (Health/Disease) of the BIRCOTEBS species.

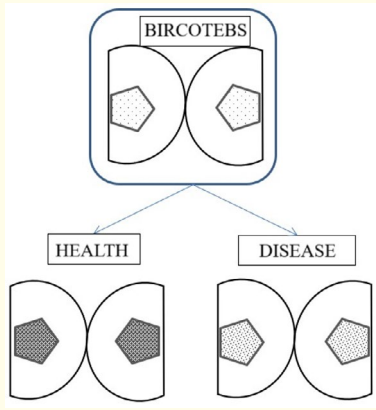

Figure 1: Bilateral radiographic conformation (BIRCOTEBS) represents the exclusive random events by which we understand the complementary states (Health/Disease) of the middle-ear mucosa depending on the corresponding species of conformation. (this figure follows and illustrates Table 5).

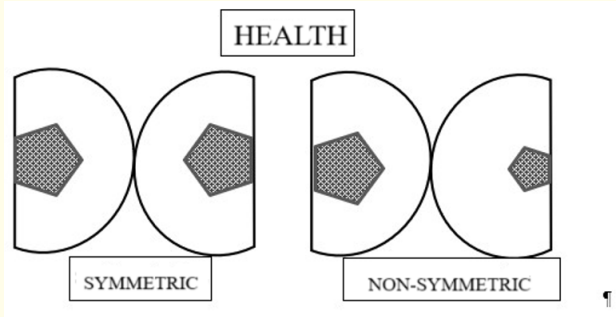

Figure 2: Sinthetic images of the radiographic conformations corresponding to the state of Health.

URCOTEBS _d, URCOTEBS _c, URCOTEBS _b, and URCOTEBS _a.

The corresponding Greek letter designates the state of disease for each of these conformations: URCOTEBS _δ, URCOTEBS _γ, URCOTEBS_β, URCOTEBS_α, and the capital letters define their state of health: URCOTEBS_D, URCOTEBS_C, URCOTEBS _B, URCOTEBS_A.

URCOTEBS_d is the smallest unilateral radiographic conformation of the TB in Schuller's projection and is, by definition, a radiographic image of the state of disease of the *D-Organ*. The probability of disease in URCOTEBS_d is 100% [1, 2].

Table IV represents the main source of data for our entire endeavor (Figure 2). By sorting and filtering the data from this table we will emphasize on the state of disease of the *D-Organ*, equivalent to the state of chronic inflammation of the ME mucosa as well as its complementary (contrary) state, the state of health (absence of disease). Both states (Health/Disease) are studied exclusively through Probability Theory and Statistics (stochastic processes) [1-3].

As far as basic notions of Health and Disease are concerned, as well as the relationship between them, it is necessary to particularize that Disease means exclusively the morbid entity previously defined as Chronic Inflammatory Disease of the Middle-ear Mucosa (CIDMM) whilst Health means the lack of said disease. This means that we shall define *stricto sensu* the complementary (contrary) state

to Middle-ear Mucosa Inflammation (lack of Middle-ear Mucosa Inflammation). This statement is exclusive for Inflammation; other diseases not related to *D-Organ* physiology may be present. The two states of the mucosa are considered random events and their genesis (probability) is detailed in Table V.

Results

Following our process of thinking, the state of Health is by definition a bilateral state of clinical facts on the basis of the bilaterality of the organ (pair organ) and it can be either symmetric or non-symmetric - see Figures 3 & 4. In Table VI-VIII we define the ratio between the prevalence of the two states, either symmetric or non-symmetric.

The identity or non-identity between the **URCOTEBS** of the two ears of the subject constitutes the criteria for the division of the two notions, Health and Disease - *Omnis divisio debet esse per opposita* (every division must be through opposites).

For the notion of Health there are two levels of division (Tables VII & VIII and Figures 3 & 4).

The first division step uses as criteria the identity or non-identity between the **URCOTEBS** that constitute the **BIRCOTEBS**. Figure 2 presents the magnitude ratio between the prevalence of these two notions which are first order species:

1. Symmetrical Health (Table VIII) -first clinical - radiographic form of the first order of the Health Status,
2. Non-symmetrical Health (Table VII) - second clinical - radiographic form of the first order of the Health Status.

For the second division step, both the criteria and the terms of division (notions which are second order species) are the combinations of the two possible **URCOTEBS** that constitute the **BIRCOTEBS**. Based on the prevalence of the notions first order species (clinical-radiographic forms of the first order) we can enunciate that the State of Health is characterized by the symmetry of the **URCOTEBS** and even more, that this state of fact is most probable in case of maximum development of *Variable Geometry Peripheral Endo-temporal Bony Cavity Complex* [1] (**URCOTEBS**_A; **BIRCOTEBS**_ A~A; relative frequency 96.63%) - see Figures 3 & 4. This fact is in accordance to all the premises - *Nullum verum inferet falsum* (Falsehood will bring no truth) [2, 3]. The two notions, which are first order species, are from a radiographic-stochastic point of view, the first order clinical forms of the Health State of the ME mucosa (*D-Organ*); the prevalences attached to these clinical-radiographic forms constitute the epidemiologic magnitude *Unilateral* and *Bilateral Disease*. These two are the clinical forms of the first order (nosographic dimension) both as formal logical divisions, into first order species of a genus and especially as definition of intensity of the pathological consequences and physical and functional prognostic. As far as prognostic information is concerned (especially functional), the magnitude ratio between the prevalence of the two clinical forms (Figures 3 & 4) pleads in favor of non-contradiction between the initial premise (Thermodynamic model of the structure and function of the ME) [3] and the natural order of things.

As previously stated, for the second stage of division for the two Disease States (uni/bilateral) - see Table IX & Figure 5, the criteria are identity/non-identity of the two **URCOTEBS** that constitute the **BIRCOTEBS** - *Omnis divisio debet esse per opposita* (every division must be by opposites).

Unilateral disease is stochastically characterized by asymmetry (Table X & Figure 6). This is yet another expression of the concordance we aim to emphasize. Finally, in the case of unilateral non-symmetric disease (Table XI & Figure 7-10), the criteria of the third division stage are precisely the concordance/non-concordance between the size of the *Variable Geometry Peripheral Endo-temporal Bony Cavity Complex and the presence/absence* of disease. Non-concordance which is the paradoxical clinical form is possible in virtue of probability calculations but its prevalence. (Table XII, XIII & Figure 10) is in itself a justification of the coherence of our explanation based on a completely defined theoretical model [2, 3]. It concerns the clinical forms of the third order of the asymmetric unilateral disease: orthodoxical (Table XIV & Figure 9) and paradoxical (Table XIII & Figure 10) and especially the ratio between their characteristic prevalences.

Bilateral disease is characterized by the symmetry of the **URCOTEBS** (Figure 6, 11, 12 & Tables XV, XVI) as shown by the ratio of the relative frequencies of the prevalence structure. The distribution of relative frequencies of **URCOTEBS** in case of symmetrical bilateral disease (Figure 11 & Table XV) draws attention on the high degree of sensitivity and specificity of the radiological examination of the TB in Schuller view in establishing a positive diagnosis. In other words, it is the expression of the previously discussed coherence (consequential materialis): ***URCOTEBS_d*** is pathognomonic (***URCOTEBS_δ***) for the Chronic Inflammatory Disease of the Middle-ear Mucosa (CIDMM) [1].

Discussions

Figures 5-12 reveal that the manifestations of **BIRCOTEBS** are divided over three or four stages through completely defined criteria, into species of the first, second, third and fourth order of the genus *CIDMM* or clinical-radiographic forms of the first, second, third and fourth order of the genus *CIDMM*.

Both **URCOTEBS** and **BIRCOTEBS** are stochastic mass phenomena (randomized exclusive events). Their essential characteristic is the relative consistency (propensity towards stability) of attainment probability. In other words, **BIRCOTEBS** constitutes a complete system of randomized (stochastic) exclusive events that can be achieved with a pair of ME (pair of *D-Organs*) of a subject (statistical unit) or of any given human statistical population. According to the law of large numbers (Moivre-Laplace) which transforms probabilities into frequencies or prevalence, we can obtain a complete picture of *CIDMM* Epidemiology.

Apart from this essential characteristic (consistency of frequency), each specific manifestation of **BIRCOTEBS** also has a precise significance for the physiologic status (Health - see Figures 2-4) or pathologic status (Disease - see Figures 5-124) of the mucosa of the pair of ME. This results in modeling the nosography of *CIDMM* based on radiological examination, probability theory and statistics (a *radiographic-stochastic-nosographic model*). The essential note in characterizing this nosography is its foundation on an objective examination method which is the comparative radiographic scan of the two TB in in Schuller's projection for any given patient.

This leads to a *radiographic-stochastic-epidemiologic-nosographic* model which completely defines 30 notions species of the genus Disease (*CIDMM*) and 8 notions species of the genus Health (absence of *CIDMM*) - see Figures 3&4. The aforementioned model is also, simultaneously, a high precision instrument to objectively establish the positive diagnosis of chronic illness of the ME mucosa (*CIDMM*).

Current Index	*BIRCOTEBS Index*	*BIRCOTEBS Index*	*Probabilities of Exclusive BIRCOTEBS Events* [1]	*Generic BIRCOTEBS symbol*	*Specific BIRCOTEBS symbol Disease/ Health*	*Product of relative URCOTEBS frequencies*[1] *Disease/Health*	*Probability of Exclusive .BIRCOTEBS Event (Prevalence) Disease/Health (product of col. Iv & col. Vii)*	*Prevalence Structure (relative frequencies)*
I	II	III	IV	V	VI	VII	VIII	IX
1	3	1	0.4943	a ~ a	A ~ A	0.961	0.481	80.94%
2	10	3	0.1101	a ~ c	A ~ C	0.804	0.0897	15.09%
3	25	8	0.0245	c ~ c	C ~ C	0.673	0.0167	2.81%
4	6	2	0.0062	a ~ b	A ~ B	0.909	0.00575	0.97%
5	19	6	0.0014	b ~ c	B ~ C	0.76	0.00107	0.18%
6	16	5	0.0001	b ~ b	B ~ B	0.859	0.00007	0.01%
Sum of columns VIII & IX							0.595	100%
							59.50%	100%

Table 6: Absolute and relative frequencies of BIRCOTEBS in the Health status of the middle-ear.

Current Index	*BIRCOTEBS Index Boală/ Sănătate.*	*BIRCOTEBS Index*	*Pobability of BIRCOTEBS Event (Product of URCOTEBS Probabilities) [1]*	*Generic BIRCOTEBS symbol*	*Specific BIRCOTEBS symbol Disease/Health*	*Product of relative URCOTEBS frequencies Disease/Health*	*Probability of Exclusive .BIRCOTEBS Events (Prevalence) Disease/Health*	*Prevalence Structure (relative frequencies)*
I	II	III	IV	V	VI	VII	VIII	IX
1	10	3	0.1101	a ~ c	A ~ C	0.804	0.0897	92.90%
2	6	2	0.0062	a ~ b	A ~ B	0.909	0.0058	6.00%
3	19	6	0.0014	b ~ c	B ~ C	0.76	0.0011	1.10%
Sum of probabilities (col.VIII&IX)							0.0965	100.00%
							9.65%	

Table 7: Radiographic Non-Symmetric Health –Clinical-radiographic form of the 1st order – 1st order species.

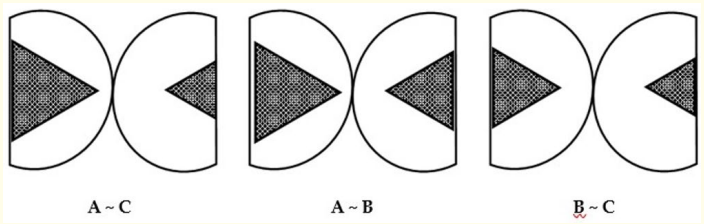

Figure 3: Schematic icons of BIRCOTEBS, in decreasing order of relative frequencies corresponding to the state of Non-symmetric Health. Clinical-radiographic form of the 1st order – 1st order species (see Table 7).

Current Index	*BIRCOTEBS Index Disease/Health.*	*BIRCOTEBS Index*	*Pobability of BIRCOTEBS Event (Product of URCOTEBS Probabilities) [1]*	*Generic BIRCOTEBS symbol*	*Specific BIRCOTEBS symbol Disease/Health*	*Product of relative URCOTEBS frequencies Disease/Health*	*Probability of Exclusive .BIRCOTEBS Events (Prevalence Disease/Health*	*Prevalence Structure (relative frequencies)*
I	II	III	IV	V	VI	VII	VIII	IX
1	3	1	0.4943	a ~ a	A ~ A	0.961	0.481	96.63%
2	25	8	0.0245	c ~ c	C ~ C	0.673	0.0167	3.36%
3	16	5	0.0001	b ~ b	B ~ B	0.859	0.0000686	0.01%
Sum of probabilities (column VIII&IX)							0.498	100%
							49.8%	

Table 8: Radiographic Symmetric Health –Clinical-radiographic form of the 1st order – 1st order species.

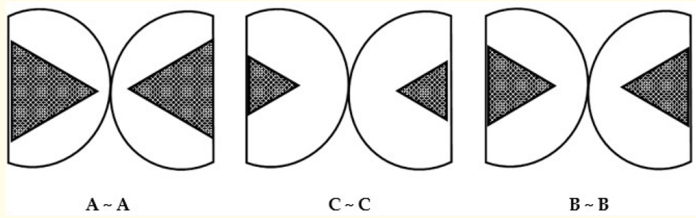

Figure 4: Schematic icons of BIRCOTEBS, in decreasing order of relative frequencies corresponding to the state of Symetric Health. Clinical-radiographic form of the 1st order – 1st order species (see Table 8).

Current Index	*BIRCOTEBS Index Disease/Health.*	*BIRCOTEBS Index*	*Pobability of BIRCOTEBS Event (Product of URCOTEBS Probabilities) [1]*	*Generic BIRCOTEBS symbol*	*Specific BIRCOTEBS symbol Disease/Health*	*Product of relative URCOTEBS frequencies Disease/Health*	*Probability of Exclusive .BIRCOTEBS Events (Prevalence) Disease/Health*	*Prevalence Structure (relative frequencies)*
I	II	III	IV	V	VI	VII	VIII	IX
1	28	10	0.0953	d ~ d	d ~ d	1.00000	0.0965000	86.80%
2	26	9	0.0483	c ~ d	g ~ d	0.18000	0.0088100	7.90%
3	12	4	0.217	a ~ d	a ~ d	0.01950	0.0042900	3.90%
4	23	8	0.0245	c ~ c	g ~ g	0.03230	0.0008040	0.72%
5	8	3	0.1101	a ~ c	a ~ g	0.00351	0.0003920	0.35%
6	21	7	0.0027	b ~ d	b ~ d	0.07310	0.0002030	0.18%
7	1	1	0.4943	a ~ a	a ~ a	0.00038	0.0001910	0.17%
8	17	6	0.0014	b ~ c	b ~ g	0.01310	0.0000185	0.02%
9	4	2	0.0062	a ~ b	a ~ b	0.00143	0.0000090	0.01%
10	14	5	0.0001	b ~ b	b ~ b	0.00534	0.0000004	0.00%
Sum of probabilities (column VIII&IX)							0.111	100.00%
							11,1%	

Table 9: Bilateral Disease – 1st order species – Clinical-radiographic form of the 1st order.

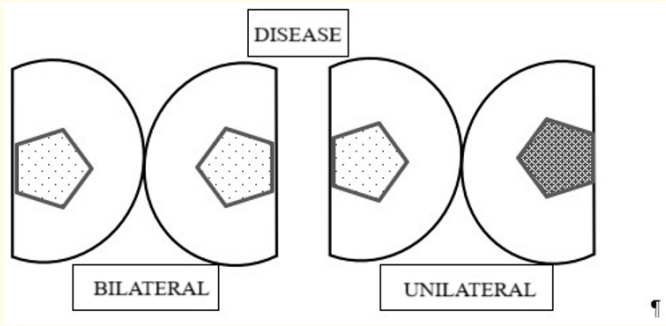

Figure 5: Schematic icons of BIRCOTEBS, corresponding to the state of Disease. (see Tables 9 & 10).

Current Index	*BIRCOTEBS Index*	*BIRCOTEBS Index*	*Pobability of BIRCOTEBS Event (Product of URCOTEBS Probabilities)* [1]	*Generic BIRCOTEBS symbol*	*Specific BIRCOTEBS symbol Disease/Health*	*Product of relative URCOTEBS frequencies Disease/Health*	*Probability of Exclusive .BIRCOTEBS Events (Prevalence) Disease/Health*	*Prevalence Structure (relative frequencies)*
I	II	III	IV	V	VI	VII	VIII	IX
1	13	4	0.217	d ~ a	δ ~ A	0.9800	0.21600000	73%
2	27	9	0.0483	d ~ c	δ ~ C	0.8200	0.04020000	14%
3	11	3	0.1101	c ~ a	γ~ A	0.1760	0.01970000	6.70%
4	2	1	0.4943	a ~ a	α ~ A	0.0191	0.00959000	3.30%
5	24	8	0.0245	c ~ c	γ ~ C	0.1480	0.00367000	1.20%
6	22	7	0.0027	d ~ b	δ ~ B	0.9270	0.00257000	0.90%
7	9	3	0.1101	a ~ c	α ~ C	0.0160	0.00179000	0.60%
8	7	2	0.0062	b ~ a	β ~ A	0.0717	0.00045300	0.15%
9	20	6	0.0014	c ~ b	γ ~ B	0.1670	0.00023500	0.08%
10	5	2	0.0062	a ~ b	α ~ B	0.0181	0.00011400	0.04%
11	18	6	0.0014	b ~ c	β ~ C	0.0600	0.00008450	0.03%
12	15	5	0.0001	b ~ b	β ~ B	0.0678	0.00000541	0.00%
Sum of probabilities (column VIII&IX)							0.294	100%
							29,4%	

Table 10: Unilateral Disease – 1st order species – Clinical-radiographic form of the 1st order.

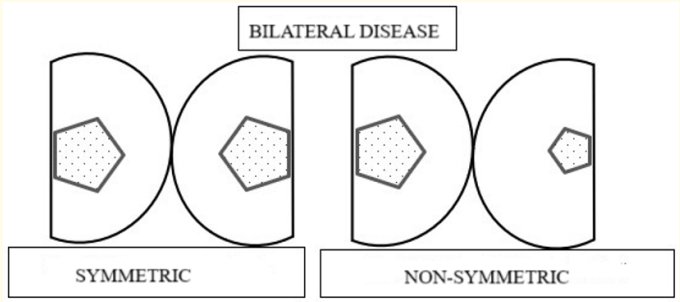

Figure 6: Schematic icons of BIRCOTEBS, corresponding to the state of Bilateral Disease. (see Tables 9 & 10).

Current Index	*BIRCOTEBS Index*	*BIRCOTEBS Index*	*Pobability of BIRCOTEBS Event (Product of URCOTEBS Probabilities)* [1]	*Generic BIRCOTEBS symbol*	*Specific BIRCOTEBS symbol Disease/Health*	*Product of relative URCOTEBS frequencies Disease/Health*	*Probability of Exclusive BIRCOTEBS Events (Prevalence) Disease/Health Product of columns IV&VII*	*Prevalence Structure (relative frequencies)*
I	II	III	IV	V	VI	VII	VIII	IX
1	13	4	0.217	d ~ a	d ~ A	0.98	0.216	76.81%
2	27	9	0.0483	d ~ c	d ~ C	0.82	0.0402	14.31%
3	11	3	0.1101	c ~ a	g ~ A	0.176	0.0197	7.01%
4	22	7	0.0027	d ~ b	d ~ B	0.927	0.00257	0.92%
5	9	3	0.1101	a ~ c	a ~ C	0.016	0.00179	0.64%
6	7	2	0.0062	b ~ a	b ~ A	0.0717	0.00045	0.16%
7	20	6	0.0014	c ~ b	g ~ B	0.167	0.00024	0.08%
8	5	2	0.0062	a ~ b	a ~ B	0.0181	0.00011	0.04%
9	18	6	0.0014	b ~ c	b ~ C	0.06	0.000085	0.03%
Sum of probabilities (column VIII&IX)							0.281	100.00%
							28.10%	

Table 11: Unilateral Non-Symmetric Disease– 2nd order species – Clinical-radiographic form of the 2nd order.

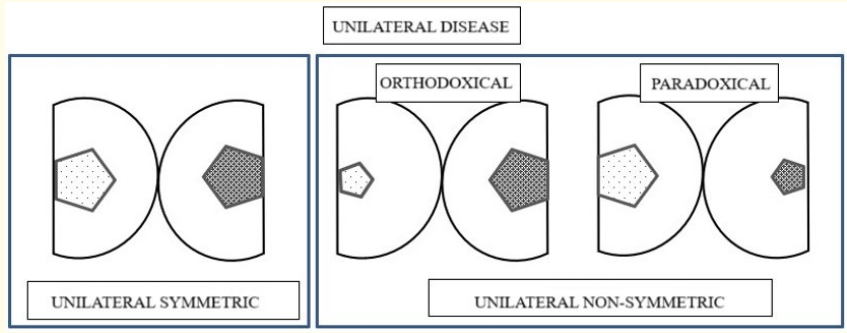

Figure 7: Schematic icons of BIRCOTEBS, corresponding to the state of Unilateral Disease. (see Tables 16).

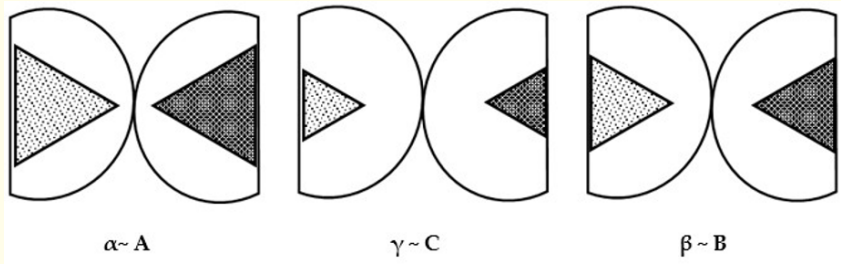

Figure 8: Schematic icons of BIRCOTEBS, in decreasing order of relative frequencies corresponding to the state of Unilateral Symmetric Disease. Clinical-radiographic form of the 2nd order – 2nd order species (see Table 16).

Current Index	*BIRCOTEBS Index*	*BIRCOTEBS Index*	*Pobability of BIRCOTEBS Event (Product of URCOTEBS Probabilities)* [1]	*Generic BIRCOTEBS symbol*	*Specific BIRCOTEBS symbol Disease/Health*	*Product of relative UR-COTEBS frequencies Disease/Health*	*Probability of Exclusive .BIR-COTEBS Events (Prevalence) Disease/Health*	*Prevalence Structure (relative frequencies)*
I	II	III	IV	V	VI	VII	VIII	IX
1	2	1	0.4943	a ~ a	a ~ A	0.0191	0.00959000	72%
2	24	8	0.0245	c ~ c	g ~ C	0.1480	0.00367000	28%
3	15	5	0.0001	b ~ b	b ~ B	0.0678	0.00000541	0.04%
Sum of probabilities (column VIII&IX)							0.0133	100%
							1.33%	

Table 12: Unilateral Symmetric Disease– 2nd order species – Clinical-radiographic form of the 2nd order.

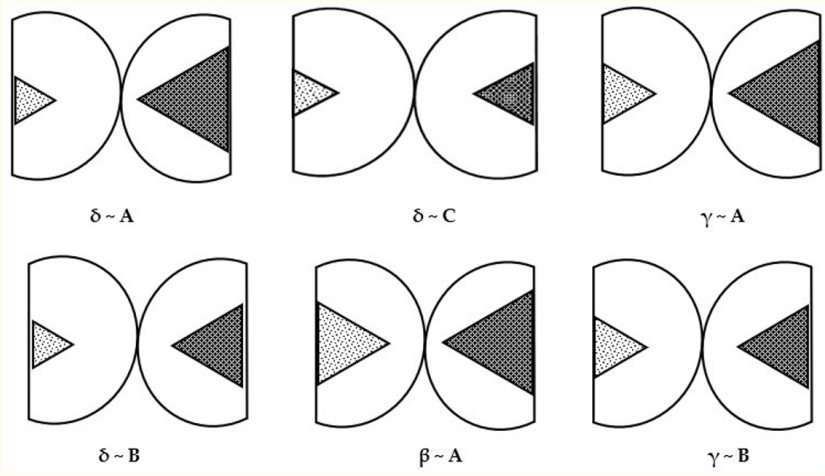

Figure 9: Schematic icons of BIRCOTEBS, in decreasing order of relative frequencies corresponding to the state of Unilateral Non-Symmetric Orthodoxal Disease. Clinical-radiographic form of the 3rd order – 3rd order species (see Table 14).

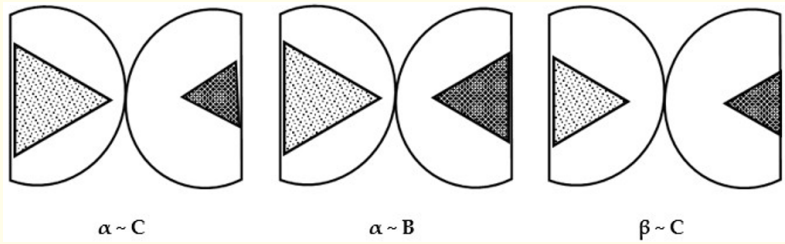

Figure 10: Schematic icons of BIRCOTEBS, in decreasing order of relative frequencies corresponding to the state of Unilateral Non-Symmetric Paradoxal Disease. Clinical-radiographic form of the 3rd order – 3rd order species (see Table 12).

Current Index	*BIRCOTEBS Index*	*BIRCOTEBS Index*	*Pobability of BIRCOTEBS Event (Product of URCOTEBS Probabilities) [1]*	*Generic BIR-COTEBS symbol*	*Specific BIR-COTEBS symbol Disease/Health*	*Product of relative URCOTEBS frequencies Disease/Health*	*Probability of Exclusive .BIR-COTEBS Events (Prevalence)= Disease/Health*	*Prevalence Structure (relative frequencies)*
I	II	III	IV	V	VI	VII	VIII	IX
1	9	3	0.1101	a ~ c	a ~ C	0.0160	0.0017900	90%
2	5	2	0.0062	a ~ b	a ~ B	0.0181	0.0001140	6%
3	18	6	0.0014	b ~ c	b ~ C	0.0600	0.0000845	4%
Sum of probabilities (column VIII&IX)							0.00199	100%
							0.199%	

Table 13: Paradoxal Unilateral Non-Symmetric Disease– 3rd order species – Clinical-radiographic form of the 3rd order.

Current Index	*BIRCOTEBS Index*	*BIRCOTEBS Index*	*Pobability of BIRCOTEBS Event (Product of URCOTEBS Probabilities)* [1]	*Generic BIRCOTEBS symbol*	*Specific BIRCOTEBS symbol Disease/Health*	*Product of relative URCOTEBS frequencies Disease/Health*	*Probability of Exclusive .BIRCOTEBS Events (Prevalence) Disease/Health*	*Prevalence Structure (relative frequencies)*
I	II	III	IV	V	VI	VII	VIII	IX
1	13	4	0.217	d ~ a	d ~ A	0.980	0.216000	77.35%
2	27	9	0.0483	d ~ c	d ~ C	0.820	0.040200	14.42%
3	11	3	0.1101	c ~ a	g ~ A	0.176	0.019700	7.06%
4	22	7	0.0027	d ~ b	d ~ B	0.927	0.002570	0.92%
5	7	2	0.0062	b ~ a	b ~ A	0.072	0.000453	0.16%
6	20	6	0.0014	c ~ b	g ~ B	0.167	0.000235	0.08%
Sum of probabilities (column VIII&IX)							0.279	100%
							27,9%	

Table 14: Orthodoxical Unilateral Non-Symmetric Disease– 3rd order species – Clinical-radiographic form of the 3rd order.

Current Index	*BIRCOTEBS Index*	*BIRCOTEBS Index*	*Pobability of BIRCOTEBS Event (Product of URCOTEBS Probabilities)* [1]	*Generic BIRCOTEBS symbol*	*Specific BIRCOTEBS symbol Disease/Health*	*Product of relative URCOTEBS frequencies Disease/Health*	*Probability of Exclusive .BIRCOTEBS Events (Prevalence) Disease/Health*	*Prevalence Structure (relative frequencies)*
I	II	III	IV	V	VI	VII	VIII	IX`
1	28	10	0.0953	d ~ d	δ ~ δ	1	0.0965	99%
2	23	8	0.0245	c ~ c	γ ~ γ	0.0323	0.000804	0.80%
3	1	1	0.4943	a ~ a	α ~ α	0.000381	0.000191	0.20%
4	14	5	0.0001	b ~ b	β ~ β	0.00534	4.27E-07	0.00%
Sum of probabilities (column VIII&IX)							0.0975	100%
							9.75%	

Table 15: Bilateral Symmetric Disease– 2nd order species – Clinical-radiographic form of the 2nd order.

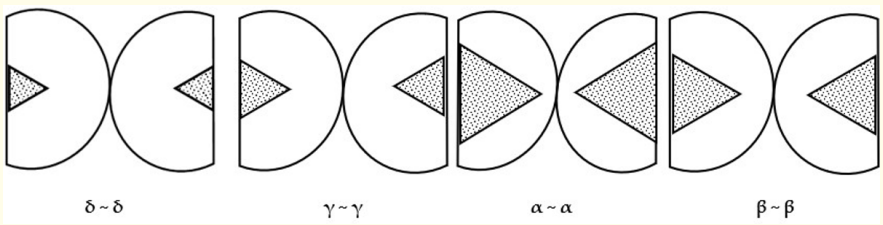

Figure 11: Schematic icons of BIRCOTEBS, in decreasing order of relative frequencies corresponding to the state of Bilateral Synmetric Disease. Clinical-radiographic form of the 2nd order – 2nd order species (see Table 15).

Current Index	*BIRCOTEBS Index*	*BIRCOTEBS Index*	*Pobability of BIRCOTEBS Event (Product of URCOTEBS Probabilities)* [1]	*Generic BIRCOTEBS symbol*	*Specific BIRCOTEBS symbol Disease/Health*	*Product of relative URCOTEBS frequencies Disease/Health*	*Probability of Exclusive .BIRCOTEBS Events (Prevalence) Disease/Health*	*Prevalence Structure (relative frequencies)*
I	II	III	IV	V	VI	VII	VIII	IX
1	26	9	0.0483	c ~ d	γ ~ δ	0.18000	0.00881000	64%
2	12	4	0.217	a ~ d	α ~ δ	0.01950	0.00429000	31%
3	8	3	0.1101	a ~ c	α ~ γ	0.00351	0.00039200	3%
4	21	7	0.0027	b ~ d	β ~ δ	0.07310	0.00020300	1%
5	17	6	0.0014	b ~ c	β ~ γ	0.01310	0.00001850	0.10%
6	4	2	0.0062	a ~ b	α ~ β	0.00143	0.00000903	0.10%
Sum of probabilities (column VIII&IX)							0.0137	100%
							1.37%	

Table 16: Bilateral Non-Symmetric Disease– 2nd order species – Clinical-radiographic form of the 2nd order.

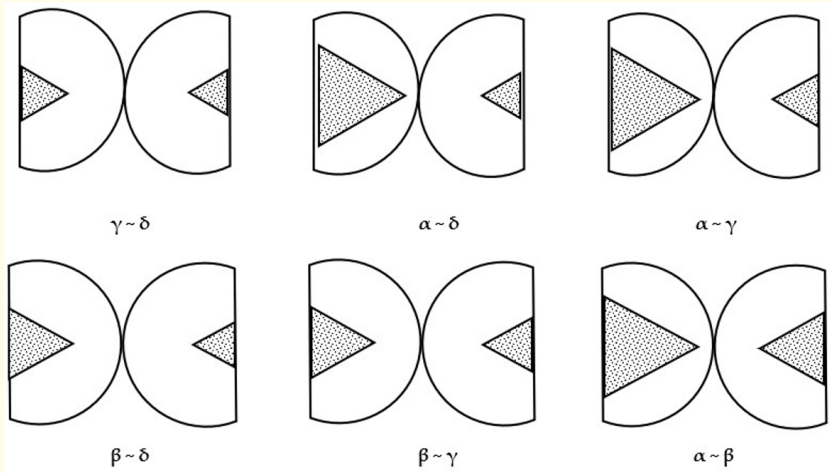

Figure 12: Schematic icons of BIRCOTEBS, in decreasing order of relative frequencies corresponding to the state of Bilateral Non-Symmetric Disease. Clinical-radiographic form of the 2nd order – 2nd order species (see Table 16).

We aim to provide a probabilistic model, not necessarily for the anatomic complexity of the middle-ear complex but rather for evaluation of Disease/Health status of said complex. The present article is only extending the previous results for **URCOTEBS** to bilateral parameters, **BIRCOTEBS**, making the statistical evaluation even more complex.

We do not intend to minimize the obvious value of moder scanning methods such as CT or MRI but we try to lay the theoretical foundations for further research which we intend to undertake in order to extend this stochastic model to three-dimensional methods. A similar model based on high resolution CT-scans of the TBs may represent a more modern method and is intended as future development of our research.

Highly technologized methods such as high-resolution computed tomography (HRCT) and non-echoplanar diffusion weighted magnetic resonance imaging (DWI) can differentiate between complex pathologies such as cholesteatoma and middle ear inflammation (MEI), infections and congenital anomalies, and also investigate the impact of post-reconstruction harmonization and data resampling with high predictive value [4-7].

Opacification in the middle ear and mastoid region can be the result of various pathological causes although it mostly reflects chronic inflammatory/infectious disease and sometimes an underlying cholesteatoma [8, 9]. Neoplastic, vascular, fibro-osseous, and traumatic changes may also occur [10]. The primary diagnostic imaging, tool is currently CT-scanning due to its exceptional spatial resolution, particularly for examining the temporal bone and ossicles. MRI complements this by offering detailed soft tissue lesion characterization and assessing involvement in the inner ear and cranial nerves [8-11].

However, we must state that classical bidimensional methods such as X-ray in Schuller's projection results in an overlapping projection of all bony cavities that comprise the General Endo-temporal Bony Cavity Complex onto the same plain (film), and this constitutes an advantage from the multiple CT sections because the set of stochastic information is found in the whole of the cavities taken as one.

For statistical and interpretation purposes, the decoding must be performed accordingly, and this occurs much faster with conventional radiography, although other imagistic methods such as CT-scan and sometimes MRI are considered the standard in today's medicine.

Many authors may consider the method as outdated and only of historic significance [12] but we consider it of interest that the use of classical radiographic methods is still in extensive use in East-European countries (and other developing countries world-wide) due to unavailability of technology and economic and financial reasons and that we have been successfully employing the **BIRCOTEBS** as an evaluation method for mastoidectomy patients for over two decades.

The suppuration of the middle-ear is a common pathology (over 20 million individuals for chronic suppuration only, according to latest reports by the WHO) facilitated by the notoriously complicated and irregular anatomic structure ot the temporal bone (TB). Clinically, the patients experience frequent recurrences and over 50% of subjects suffer from conductive hearing loss (hearing impairment) which is a serious problem confronting the otologist [13-15]. The geometry of the mastoid air cells system (MACS) has not been described for adults over a large range of MACS volumes [16]. However, the common conclusion of recent studies is that MACS volumes are indirectly related to predisposition for middle-ear pathology such as chronic otitis media [17-21]. The relationship between TB pneumatization and gas volumes within the ME represents an interesting research area as current studies tend to suggest that MACS and not the Eustachian tube opening is the primary gas source for the ME [1-3, 22, 23].

The volume of this complicated system of interconnected air cells is difficult to measure, which is why various methods [24-26] such as water-weight method, pressurized transducer method, planimetric [21, 27-30] and volumetric [26-28, 31-34]. methods have been employed. Swarts et al. and Colhoun et al. [16, 35] use Schuller projection X-rays and reconstructions from CT sections to demonstrate the linear function that correlates MACS surface area and MACS volume with a high correlation coefficient ($r \approx 0.77$ and $r \approx 0.95$ respectively). The conclusion of all this research is that relatively simple X-ray procedures can be used to screen ears for MACS volume [1, 16].

The middle-ear with its mastoid air cell system and ossicular chain represents a complex anatomic system which requires advanced and complex mathematical models (static and dynamic behaviors) for function assessment. These methods have been based on deterministic approaches [36-40], lumped element models, distributed parameter models, multi-body systems, finite element models [41, 42] for evaluation of healthy ME as well as pathological conditions [43] and verification of functional ossicular chain reconstruction results [44, 45].

As stated in our previous studies regarding unilateral stochastic models of the TB [1], the high degree of variability amongst individuals leads to large discrepancies among samples. This means that the ME behaves as an uncertain system which makes stochastic models very useful [36, 46]. Modeling a dynamical system with uncertainties has been presented in the literature (47) and employes

two groups of methods: parametric and nonparametric [36, 47, 48].

Statistical calibration has also been used on geometry-based models such as the finite element (FE) model to calculate dynamic characteristics of the middle-ear [1, 41, 49-52].

As presented in the initial URCOTEBS article [1], the tables and graphical represent-tations are indeed complex and sometimes complicated but stochastic analysis usually is. The data may look daunting for a medical professional and we consider this as the main limit of the present work as it is not intended primarily for physicians but rather for mathematicians, statisticians and physics specialist with an extension to-wards the medial professionals (physiopathologists, anatomists, ENT specialists, radiologists) that may also possess the mathematical knowledge to understand the possible practical uses of the research. A more clinically oriented presentation based on our extensive experience with this evaluation method will follow in future research.

Clinical scenarios intended for validation of our model as well as a possible flowchart depicting the model's clinical applicability will be part of this future research.

The authors also plan to extend and somehow systematize the clinical application of these statistical tables as part of our future research that will use computer software for automatic interpretation.

Conclusion

The *D-Organ* gives us a unique opportunity to study it and its most essential aspects through radiological examination. The **BIRCOTEBS** is the theoretical and practical-experimental basis of modeling the nosography for Chronic Inflammatory Disease of the Middle-ear Mucosa (*CIDMM*). This *nosographic-radiographic-stochastic model* (both in theory and in practice - the patient's radiography) represents a necessary but not sufficient step in defining all aspects of chronic ME disease.

We aim to continue our research and to tap the considerable potential of this statistic-probabilistic perspective on the phenomena and processes of interest regarding the structure and function of the ME, both in normal and pathological conditions.

The *nosographic - radiologic - stochastic model* we discussed simultaneously constitutes a *theoretical epidemiologic-statistic model* as the calculated probabilities for each species of **BIRCOTEBS** are being transformed according to the law of large numbers (Moivre-Laplace) into absolute frequences which in Epidemiology are known as prevalence.

We must not overlook the rigorous theoretical foundation of our endeavor. It is based on the hypothesis of the existence of the *D-Organ* which can explain in a coherent, exhaustive and non-contradictory manor the pathology and clinical manifestations of the *CIDMM*. The present work is but a step towards justifying this statement.

As previously stated by the American mathematician *Warren Weaver* (*1894-1978*), probabilistic logic can consider an entire array of statements, of which none entirely false nor entirely true and order them in relation to their degree of truth, determining how much more probable one is compared to the other. This method does not limit itself to binary values of 0 and 1 but utilizes an infinity of values in the form of numbers situated between 0 and 1.

Probability theory can analyze situations where the scarcity of information prevents us from applying classical logic and is capable of providing the best answer justified by incomplete information. If we understand that the most basic laws of elementary physical phenomena are probabilistic, we can acknowledge that probability theory is essential for many special scientific fields, including medicine. In a large number of instances, it does not only offer advice on a solution but also the degree of reliability of said advice.

References

1. RAdulescu M., et al. "Defining the URCOTEBS system as a unilateral radiographic-stochastic model for the complementary states (health/disease) of the D-organ and middle-ear mucosa". Applied Sciences 13 (2023): 12861.

2. RAdulescu M., et al. "Geometric-statistical model for middle-ear anatomy and ventilation". Applied Sciences 12 (2022): 11287.
3. RAdulescu M, Mocanu H, Nechifor A and Mocanu AI. "Thermodynamic model for middle-ear ventilation: Defining the D-organ by comparison to the Eustachian tube (Re-interpretation of a classic experiment and review of literature)". Acta Technica Napocensis, Series: Applied Mathematics, Mechanics and Engineering 65.1 (2022): 69-78.
4. Arendt CT., et al. "Radiomics of high-resolution computed tomography for the differentiation between cholesteatoma and middle ear inflammation: Effects of post-reconstruction methods in a dual-center study". European Radiology 31 (2021): 4071-4078.
5. Thukral CL., et al. "Role of high-resolution computed tomography in evaluation of pathologies of temporal bone". Journal of Clinical and Diagnostic Research 9.9 (2015): TC07-TC10.
6. Lingam RK., et al. "Non-echoplanar diffusion weighted imaging in the detection of post-operative middle ear cholesteatoma: Navigating beyond the pitfalls to find the pearl". Insights into Imaging 7 (2016): 669-678.
7. van Egmond SL., et al. "A systematic review of non-echo planar diffusion-weighted magnetic resonance imaging for detection of primary and postoperative cholesteatoma". Otolaryngology-Head and Neck Surgery 154 (2016): 233-240.
8. Mahdavi A. "Diagnostic and imaging findings in inflammatory opacifications of the middle ear: A review of the literature". International Tinnitus Journal 27.2 (2024): 146-153.
9. Lemmerling MM., et al. "Imaging of the opacified middle ear". European Journal of Radiology 66.3 (2008): 363-371.
10. Lo AC and Nemec SF. "Opacification of the middle ear and mastoid: Imaging findings and clues to differential diagnosis". Clinical Radiology 70.5 (2015): e1-e13.
11. Mafee MF. "MRI and CT in the evaluation of acquired and congenital cholesteatomas of the temporal bone". Journal of Otolaryngology 22.4 (1993): 239-248.
12. Sadé J and Hadas E. "Prognostic evaluation of secretory otitis media as a function of mastoidal pneumatization". Archives of Otorhinolaryngology 225 (1979): 39-44.
13. Mocanu H and Oncioiu I. "The influence of clinical and environmental risk factors in the etiology of congenital sensorineural hearing loss in the Romanian population". Iranian Journal of Public Health 48 (2019): 2301-2303.
14. Mocanu H. "The role of perinatal hearing screening in the normal development of the infant's language". In Debating Globalization. Identity, Nation and Dialogue. 4th Edition (2017): 562-569.
15. Mocanu H. "The economic impact of early diagnosis of congenital hearing loss". In Debating Globalization. Identity, Nation and Dialogue. 4th Edition (2017): 556-561.
16. Swarts JD, Cullen Doyle BM and Doyle WJ. "Surface area-volume relationships for the mastoid air cell system in adult humans". Journal of Laryngology and Otology 125.6 (2011): 580-584.
17. Sade J and Fuchs C. "A comparison of mastoid pneumatization in adults and children with cholesteatoma". European Archives of Otorhinolaryngology 251 (1994): 191-195.
18. Sade J and Fuchs C. "Secretory otitis media in adults: I. The role of mastoid pneumatization as a risk factor". Annals of Otology, Rhinology & Laryngology 105 (1996): 643-647.
19. Sade J and Fuchs C. "Secretory otitis media in adults: II. The role of mastoid pneumatization as a prognostic factor". Annals of Otology, Rhinology & Laryngology 106 (1997): 37-40.
20. Lesinskas E. "Factors affecting the results of nonsurgical treatment of secretory otitis media in adults". Auris Nasus Larynx 30 (2003): 7-14.
21. Valtonen HJ., et al. "Development of mastoid air cell system in children treated with ventilation tubes for early-onset otitis media: A prospective radiographic 5-year follow-up study". Laryngoscope 115 (2005): 268-273.
22. Doyle WJ. "The mastoid as a functional rate-limiter of middle ear pressure change". International Journal of Pediatric Otorhinolaryngology 71 (2007): 393-402.
23. Cohen D., et al. "Ventilation and clearance of the middle ear". Journal of Laryngology and Otology 123 (2009): 1314-1320.
24. Byun SW., et al. "Normal mastoid air cell system geometry: Has surface area been overestimated?" Clinical and Experimental Otorhinolaryngology 9.1 (2016): 27-32.
25. Park MS, Yoo SH and Lee DH. "Measurement of surface area in human mastoid air cell system". Journal of Laryngology and Otol-

ogy 114.2 (2000): 93-96.

26. Koc A., et al. "Evaluation of the mastoid air cell system by high resolution computed tomography: Three-dimensional multiplanar volume rendering technique". Journal of Laryngology and Otology 117.8 (2003): 595-598.
27. Palva T and Palva A. "Size of the human mastoid system". Acta Otolaryngologica 62 (1966): 237-251.
28. Csakanyi Z., et al. "Volume and surface of the mastoid cell system in otitis media with effusion in children: A case-control study by three-dimensional reconstruction of computed tomographic images". Otology & Neurotology 32.1 (2011): 64-70.
29. Cinamon U. "The growth rate and size of the mastoid air cell system and mastoid bone: A review and reference". European Archives of Otorhinolaryngology 266 (2009): 781-786.
30. Hug JE and Pfaltz CR. "Temporal bone pneumatization: A planimetric study". Archives of Otorhinolaryngology 233 (1981): 145-156.
31. Flisberg K and Zsigmond M. "The size of the mastoid air cell system: Planimetry-direct volume determination". Acta Otolaryngologica 60 (1965): 23-29.
32. Todd NW, Pitts RB, Braun IF and Heindel H. "Mastoid size determined with lateral radiographs and computerized tomography". Acta Otolaryngologica 103 (1987): 226-231.
33. Vrabec JT., et al. "3D CT imaging method for measuring temporal bone aeration". Acta Otolaryngologica 122 (2002): 831-835.34.
34. Lee DH., et al. "Volume variation of mastoid pneumatization in different age groups: A study by three-dimensional reconstruction based on computed tomography images". Surgical and Radiologic Anatomy 27 (2005): 37-42.
35. Colhoun EN., et al. "A comparison between area and volume measurements of the mastoid air spaces in normal temporal bones". Clinical Otolaryngology and Allied Sciences 13 (1988): 59-63.
36. Lobato LC, Paul S and Cordioli JA. "Stochastic model of the human middle ear using a nonparametric probabilistic approach". Journal of the Acoustical Society of America 151.3 (2022).
37. De Greef D., et al. "Details of human middle ear morphology based on micro-CT imaging of phosphotungstic acid-stained samples". Journal of Morphology 276.9 (2015): 1025-1046.
38. Rosowski JJ, Ravicz ME and Merchant SN. "Testing a method for quantifying the output of implantable middle ear hearing devices". Audiology and Neurotology 12 (2007): 265-276.
39. Funnell WRJ, Maftoon N and Decraemer WF. "Modeling of middle ear mechanics". In Modeling of Middle Ear Mechanics. Springer: New York (2013): 171-210.
40. Paolis AD., et al. "Analytical and numerical modeling of the hearing system: Advances towards the assessment of hearing damage". Hearing Research 349 (2017): 111-128.
41. Koike T, Wada H and Kobayashi T. "Modeling of the human middle ear using the finite-element method". Journal of the Acoustical Society of America 111.3 (2002): 1306-1317.
42. Lobato L, Paul S and Cordioli J. "Statistical analysis of the human middle ear mechanical properties". Journal of the Acoustical Society of America 151.3 (2022): 2043-2054.
43. Gan RZ., et al. "Finite element modeling of sound transmission with perforations of tympanic membrane". Journal of the Acoustical Society of America 126.1 (2009): 243-253.
44. Neudert M., et al. "Feasibility study of a mechanical real-time feedback system for optimizing the sound transfer in the reconstructed middle ear". Otology & Neurotology 39.10 (2018): e907-e920.
45. Mocanu H., et al. "Evaluation of Vibrant® Soundbridge™ positioning and results with laser Doppler vibrometry and the finite element model". Experimental and Therapeutic Medicine 21 (2021): 262.
46. Ebrahimian A and Maftoon N. "Stochastic finite element modelling of human middle-ear". CMBES Proceedings 44 (2021).47. Daouk S., et al. "Uncertainties in structural dynamics: Overview and comparative analysis of methods". Mechanics & Industry 16.4 (2015): 404.
47. Soize C. "A nonparametric model of random uncertainties for reduced matrix models in structural dynamics". Probabilistic Engineering Mechanics 15.3 (2000): 277-294.
48. Lee D and Ahn TS. "Statistical calibration of a finite element model for human middle ear". Journal of Mechanical Science and

Technology 29.7 (2015): 2803-2815.

49. Volandri G., et al. "Model-oriented review and multi-body simulation of the ossicular chain of the human middle ear". Medical Engineering & Physics (2012).
50. Gan R, Reeves B and Wang X. "Modeling of sound transmission from ear canal to cochlea". Annals of Biomedical Engineering 35 (2007): 2180-2195.
51. Gan RZ., et al. "Acoustic structural coupled finite element analysis for sound transmission in human ear—Pressure distributions". Medical Engineering & Physics 28 (2006): 395-404.